Adv. Polar Upper Atmos. Res., **15**, 43-60, 2001

Distortion of the nightside boundary of the "firmly-closed" region in the 1996 Tsyganenko magnetic field model

Takashi Yamamoto[1], Shoshi Inoue[2] and Masao Ozaki[3]

[1] *Department of Earth and Planetary Physics, University of Tokyo, Hongo 7-chome, Bunkyo-ku, Tokyo 113-0033*
[2] *Faculty of Education, Iwate University, Morioka, Iwate 020-8550*
[3] *Institute of Industrial Science, University of Tokyo, Roppongi 7-chome, Minato-ku, Tokyo 106-8558*

Abstract: This paper proposes that the outer boundary of the "firmly-closed" region should be represented by field lines with the adiabaticity parameter, κ, equal to unity at the equator, where κ^2 is the ratio between the radius of the field-line curvature and the Larmor radius of an ion with 1 keV of energy. Just outside the boundary where $\kappa = 1$, plasma particles (primarily ions) can be nonadiabatically accelerated in the presence of the dawn-to-dusk electric field. An inwardly convecting flux tube will attain the maximum content of nonadiabatically accelerated particles when it passes the $\kappa \sim 1$ boundary. Thus, the $\kappa = 1$ boundary outlines the region of the plasma population with a maximum content of nonadiabatically accelerated particles. In addition, the field lines with $\kappa = 1$ are shown to have a minimum field strength of roughly 1 nT at the equator. From this fact, a field line with $\kappa < 1$ may not be considered as being "firmly-closed" in the sense that such a field line may easily merge with an interplanetary field line. The outer boundary of the nightside firmly-closed region in the Tsyganenko model has an IMF B_Z dependence that is consistent with observations. Moreover, this boundary is found to be "distorted", favoring the generation of region 1 field-aligned currents.

1. Introduction

Several authors (*e.g.*, Birn *et al.*, 1991; Elphinstone *et al.*, 1991; Nishitani, 1992) have attempted to determine the outer (higher L values) boundary of the closed region of the Earth magnetosphere, using the Tsyganenko magnetic field models (Tsyganenko, 1987, 1989). In these reports, the boundaries were simply defined as those traced along the field lines to some specific *a priori* limit in the tail region. For a review of these works, see the introduction of Yamamoto *et al.*, 1999a (hereafter referred to as Y99). Y99 introduced a new definition of the outer boundary of the (nightside) "firmly-closed" closed region. This boundary was defined as consisting of the field lines along which the magnetic field strength, B, drops to a critical level, B_c, of a few nanoteslas or less. If the magnetic field strength along a field line drops below B_c, the field line tends to merge with a field line that originates from the solar wind, *i.e.*, an interplanetary field line, since the amplitude of the fluctuating magnetic fields in the solar wind is normally of the order of 1 nT. Hence, field lines where $B_c < 1$ nT cannot be regarded as being "firmly-closed". All field lines inside the outer boundary of the firmly-closed region are

supposed to be invariably closed, since they are unperturbed by temporal fluctuations of the interplanetary magnetic field (IMF), which have amplitudes of the order of 1 nT. Notably, according to such open/closed demarcation, the polar cap could be found on the nightside polar ionosphere when the IMF is weakly northward, *i.e.*, B_Z is a few nanoteslas. (In this paper, the polar cap is defined as being encircled by the outer boundary of the firmly-closed region.) This idea is consistent with satellite observations of particle precipitation during such IMF conditions (*e.g.*, Makita *et al.*, 1988). When conventional open/closed demarcation based on a neutral line are used, however, no nightside open region is predicted because the neutral line is not formed in the magnetotail region when the IMF B_Z is appreciably above zero.

The present paper redefines the outer boundary of the nightside firmly-closed region in an attempt to establish an open/closed criterion that is more appropriate for use with injection boundaries. Here, the outer boundary is defined as consisting of the field lines with the parameter of adiabaticity (Büchner and Zelenyi, 1989; Ashour-Abdalla *et al.*, 1995), κ, equal to unity at the equator, where κ^2 gives the ratio between the radius of the field-line curvature and the Larmor radius of an ion with 1 keV of energy. (Perpendicular energy $mv_\perp^2/2$ is 2/3 keV, where m is the ion mass and $v_\perp$ is the velocity component perpendicular to the magnetic field.) Just outside of the boundary where $\kappa = 1$, plasma particles (primarily ions) can be nonadiabatically accelerated in the presence of the dawn-to-dusk electric field. Around the $\kappa = 1$ boundary, an inwardly convecting flux tube is assumed to attain the maximum content of nonadiabatically accelerated particles. Thus the $\kappa \approx 1$ boundary outlines the region of the plasma population that has the maximum content of nonadiabatically accelerated particles. In this paper, the outer boundary of the nightside firmly-closed region is numerically determined using the 1996 Tsyganenko model (Tsyganenko, 1995; Tsyganenko and Stern, 1996), which is hereafter referred to as the (original) T96 model. Practically, as will be shown in Section 3, the boundary determined using the criterion of $\kappa = 1$ is generally close to the boundary determined using $B_c = 1$ nT. (This reflects the fact that the field-line curvature does not much change along the equicontour of $B_c = 1$ nT.) Therefore, as stated above, a field line where $\kappa < 1$ will easily merge with a field line originating from the solar wind with magnetic field fluctuations of ≈ 1 nT in amplitude. In other words, the field lines where $\kappa < 1$ cannot be regarded as being "firmly-closed". For simplicity, the phrase "firmly-closed region" is often abbreviated to "closed region".

Another important finding of Y99 is that the ionospheric projection of the average magnetic drift velocity of an isotropic ion fluid has an equatorward component on the duskside of the outer boundary of the closed region and a poleward component on its dawnside, respectively. This fact can be regarded as a signature of the convection-distortion of that boundary, which was earlier suggested as a possible generation mechanism for the nightside region 1 field-aligned current (FAC) (Yamamoto *et al.*, 1996; Yamamoto and Inoue, 1998). Assuming an (inward) gradient of the energy density of the plasma particles near the outer boundary of the closed region, Y99 estimated the intensity of the region 1 FAC that would be generated at this location. The estimated value was comparable to observed values.

The main purpose of the present paper is to demonstrate the IMF B_Z dependence of the distortion of the outer boundary of the nightside closed region, using the T96 model.

The distortion occurs for all ranges of the model parameters examined in the present study (probably for any physically probable situation) as long as the polar cap exists, where the polar cap is defined as being encircled by the $\kappa=1$ boundary. If the IMF B_Z is less than a few nanoteslas (although this critical value depends on other parameters in the model), the distortion is sufficient to produce a region 1 field-aligned current of observable intensity. As the IMF B_Z decreases, the distortion becomes more significant, producing more intense region 1 currents while the polar cap expands.

2. Modification of the T96 model

The terrestrial magnetic field assumed in the present paper is a combination of the dipole field, the field originating from the extraterrestrial current source modeled by Tsyganenko (1995) and Tsyganenko and Stern (1996), and the additional uniform field representing the IMF penetration into the magnetosphere. Hereafter, the combination of the first two components is referred to as the original T96 model. This section gives a brief description of the original T96 model as well as the reason for modifying it by the addition of the above-mentioned third component.

The magnetic field configuration in the original T96 model is parametrized by the IMF B_Y and B_Z components, the solar wind dynamic pressure, $P_{\rm dyn}$, and the $D_{\rm ST}$ index. (In this paper, the solar-magnetospheric coordinates (X, Y, Z) are used.) In principle, this parametrization allows one to study the properties of the terrestrial magnetic field that are dependent on these parameters in wide numerical ranges. However, statistical field models are usually expected to provide a good description of the actual magnetosphere during quiet to moderately-disturbed periods, rather than severely disturbed ones (*e.g.*, with $K_P>4$). The reason for this is that the distribution of plasma particles, the magnetospheric/ionospheric currents and the electric/magnetic fields are all so changeable, both temporally and spatially, during disturbed periods, that it may be inappropriate to apply a statistical model to such a magnetospheric state. Therefore, this study focuses on cases with relatively small magnitudes of IMF B_Z, $P_{\rm dyn}$ and $D_{\rm ST}$ (<0). The effects of IMF B_Y and dipole tilt are not considered; they are set at zero. (The IMF B_Y dependence of the outer boundary of the closed region will be investigated in the near future.) The magnetic field described in this paper thus has the following basic characteristics: (1) The magnetic field at the equator, $\boldsymbol{B}_{\rm eq}$, has only a Z-component because the field lines in a model that does not consider dipole tilt are symmetric with respect to the X-Y plane. (2) At least in the tail region, the magnitude of $\boldsymbol{B}_{\rm eq}$ gives the minimum strength of $\boldsymbol{B}$ along a geometrically closed field line. (3) The field lines are also symmetric with respect to the Z-X plane, because of the absence of an IMF B_Y component. (For this reason, only the duskside halves of the two-dimensional plots of various quantities on the equatorial and ionospheric planes are shown in this paper, with the exception of Figs. 7 and 9a.)

In the original T96 model, the interplanetary magnetic field penetrating the magnetosphere is even smaller on the nightside than on the dayside. For this reason, the following features appear. (1) Even if the IMF B_Z is less than -5 nT, a neutral line is not formed in the tail region of $-150\,R_E<X$, where R_E is the Earth radius. (2) Even if the IMF B_Z increases to even greater than 5 nT, a wide open region (radius of ~10

degrees in latitude) remains on the ionosphere. These facts are exemplified by Figs. 1 and 2. Figure 1 shows the profile of the Z-component of B_{eq}, $B_{eq}(X)$, along the X-axis on the equatorial plane for IMF $B_Z=-10$, -5, 0, 5 and 10 nT, in the case of $P_{dyn}=1$ nPa and $D_{ST}=-20$ nT. The magnetic field B_{eq} (X) is positive in a wide range of $-150\,R_E<X$, meaning that a neutral line is not formed in the middle to near-Earth tail. Figure 2 shows the ionospheric projection of equicontours of $B_{eq}=0.1$ and 0.01 nT on the equatorial plane in the case of IMF $B_Z=10$ nT, $P_{dyn}=1$ nPa and $D_{ST}=-20$ nT. (Lines of $B_{eq}=0.1$ and 0.01 nT on the equatorial plane are mapped along the field lines onto the ionosphere. Hereafter, these lines are simply referred to as the $B_{eq}=0.1$ line and the $B_{eq}=0.01$ line, either on the equatorial or ionospheric plane.) On the equatorial plane, the $B_{eq}=0.01$ line is quite close to the neutral line. On the ionospheric plane, the proximity of the $B_{eq}=0.1$ line to the $B_{eq}=0.01$ line, as shown in Fig. 2, implies that the $B_{eq}=0.01$ line practically represents the (virtual) ionospheric projection of the neutral line, namely the $B_{eq}=+0$ line in the limit of $B_{eq}\to+0$. Consequently, in Fig. 2 any field line emanating from the ionospheric region surrounded by the $B_{eq}=0.01$ line (except for points very near the line) will not reach the equatorial tail region; in other words, the region inside the $B_{eq}=0.01$ line may be regarded as open.

The above-mentioned features (1) and (2) in the original T96 model are inconsistent with satellite observations (*e.g.*, Lin *et al.* (1991) is inconsistent with (1); Makita *et al.* (1988) is inconsistent with (2)). To ensure that the model conforms with observations, the penetration of IMF B_Z into the tail region must be enhanced. In the present study, a small fraction of the IMF B_Z, which is a parameter in the original T96 model, is uniformly added to the original model field. This additional component of IMF penetration is designated as B_Z^e. In the modified model that includes B_Z^e, the neutral line is formed in the near-Earth or middle tail when the IMF B_Z is below minus a few nanoteslas and the polar cap almost disappears when the IMF B_Z exceeds several nanoteslas (see Section 3). Throughout this work, the ratio of B_Z^e to IMF B_Z is fixed at 0.15, unless otherwise stated.

Finally, a brief comment is made on the validity of the linear superposition of a small fraction of the IMF on the magnetospheric field as an effect of the IMF penetration into the magnetosphere. The IMF can influence the magnetic field inside the magnetosphere by direct and indirect ways. Since the magnetosphere is exposed to the IMF maintained by the global current system configured in the solar wind, application of the Biot-Savart law shows that the magnetic field inside the magnetosphere must be described by the addition of the IMF to the fields originating from currents on the magnetopause and inside the magnetosphere as well as the Earth. (The induced field is neglected for the steady magnetosphere-solar wind interactive system.) However, the magnetosphere will diamagnetically respond to the IMF, acting to reduce the IMF inside it by changing the magnetopause and magnetospheric currents. Since such diamagnetic responses are complicated, one may examine the results from the global MHD simulation of the IMF effect on the magnetosphere to obtain a general perspective. For example, Usadi *et al.* (1993) simulated the dynamics of the magnetosphere in response to a change in the IMF from $B_Z=0$ to -5 nT. About one hour after the southward turning of the IMF at $X=20\,R_E$, the B_Z at the equator (on the Sun-Earth line) remained positive in the middle to distant tail region, although a reconnection

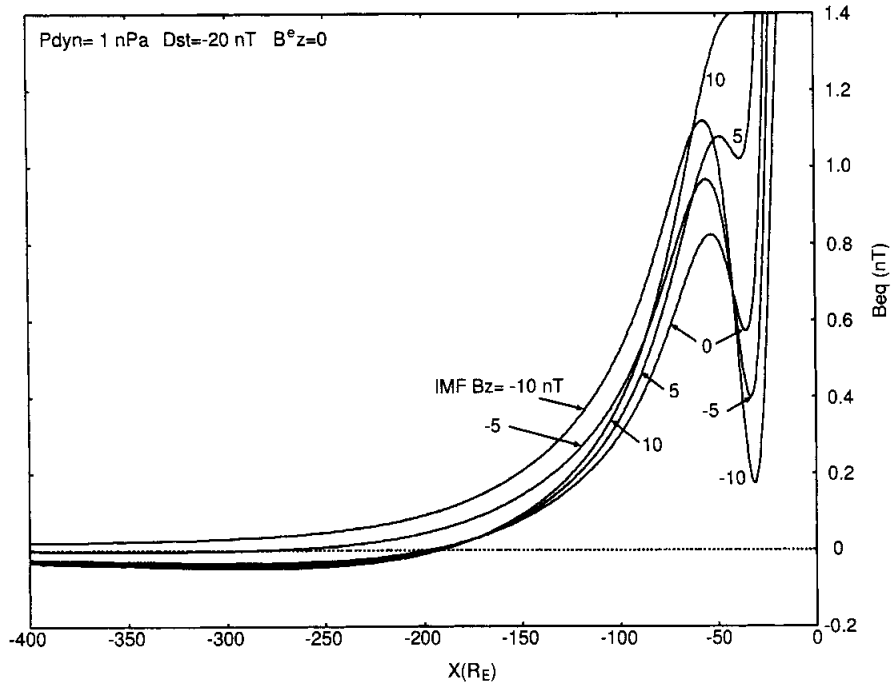

Fig. 1. Profile of the Z-component of B_{eq}, $B_{eq}(X)$, along the X-axis on the equatorial plane for IMF $B_Z = -10$, -5, 0, 5 and 10 nT, in the case of $P_{dyn} = 1$ nPa and $D_{ST} = -20$ nT. The original T96 model is used (i.e., $B^e_Z = 0$).

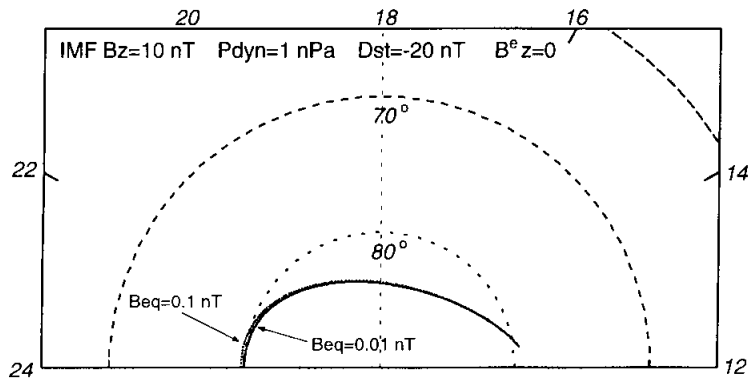

Fig. 2. Ionospheric projection of equicontours of $B_{eq} = 0.1$ and 0.01 nT on the equatorial plane, where IMF $B_Z = 10$ nT, $P_{dyn} = 1$ nPa and $D_{ST} = -20$ nT. The original T96 model is used (i.e., $B^e_Z = 0$).

occurred in the near-Earth tail. About one hour later, the B_Z at the equator was negative throughout an extended region of $-90\,R_E$ (simulation boundary) $< X \lesssim -20\,R_E$, implying that a roughly uniform penetration of IMF B_Z into the middle to distant tail had occurred with a penetration rate of $\approx 10\%$. This simulation also shows

that the B_Z at the equator is maintained above 1 nT in the tail about two hours after the northward turning to $B_Z = 5$ nT. Thus, a small fraction of the IMF B_Z can probably evenly pervade the tail region in an asymptotically steady state. As for the penetration of IMF B_Y, Fairfield (1979) showed by observations that about 13% of the IMF B_Y penetrates the magnetotail. Cowley and Hughes (1983) found that, on average, 28% of the IMF B_Y appears at geostationary orbit. From these theoretical and observational findings, the IMF B_Z penetration rate of 15% ($B_Z^* = 0.15 \times$ IMF B_Z) used in the present work may be reasonable as a lowest approximation of the IMF effect, as long as the application of the model is limited to the study of the magnetosphere that has been immersed in a steady IMF for at least a few hours.

3. Outer boundary of the firmly-closed region

Figures 3a and 3b show the equicontours of B_{eq} and κ (defined in section 1), respectively, on the equatorial X-Y plane for the case of IMF $B_Z = -4$ nT, $P_{dyn} = 1$ nPa and $D_{ST} = -20$ nT. The location of the magnetopause, which is dependent only on P_{dyn} in the T96 model, is also indicated. In Fig. 3a, the neutral line is positioned at $-80 \lesssim X(R_E) < -70$. Note that without the additional penetration of IMF B_Z, the neutral line is positioned around $X \approx -250\,R_E$ in the far distant tail (see Fig. 1). If a larger penetration is used (for example, a B_Z^* value equivalent to 30% of the IMF B_Z), the neutral line is formed in the near-Earth tail for the above-mentioned case of IMF $B_Z = -4$ nT. The B_{eq} equicontours for the case of 30% penetration can be obtained by subtracting 15% of 4 nT from the B_{eq} values in Fig. 3a. Hence, the $B_{eq} = 0.6$ line in Fig. 3a would correspond to the neutral line for the 30% penetration.

Figure 4a shows the ionospheric footprints of the $B_{eq} = 0.5$ and 1.0 nT lines, while Fig. 4b shows those of the $\kappa = 0.5$ and 1.0 lines; the footprints are obtained by mapping the equicontours in Figs. 3a and 3b, along the field lines, onto the ionospheric plane. As is noted in Section 1, the $\kappa = 1.0$ line is generally close to the $B_{eq} = 1.0$ nT line because the field-line curvature does not much change along this B_{eq} equicontour. The present paper assumes that the outer boundary of the firmly-closed region consists of the field lines where $\kappa = 1.0$. The $\kappa = 1$ line in Fig. 4b is thus the ionospheric footprint of the outer boundary of the closed region. Here it should be emphasized that the closed region predicted from the neutral line is inconsistent with satellite observations. Figure 1 (from the original T96 model) indicates that a neutral line cannot be formed in any region if only a small IMF B_Z of ~0.05 nT penetrates the tail region. It follows that the (nightside) open region disappears on the ionosphere under the condition of weakly northward ($B_Z \approx 1$ nT) IMF. This result disagrees with observations that during such IMF periods, a distinct area is present, in which the electron precipitation except for the polar rain is absent (Makita *et al.*, 1988).

Figures 5 and 6 show the IMF B_Z dependence of the polar cap, *i.e.*, the ionospheric footprint of the outer boundary of the firmly-closed region. The outer boundary is found to shift toward the lower latitudes as the IMF B_Z decreases. Namely, the polar cap expands with decreasing IMF B_Z. This result is consistent with the characteristics of the polar cap inferred from satellite observations of particle precipitation (*e.g.*, Akasofu *et al.*, 1992). In Figs. 5 and 6, the polar cap can be identified even when the

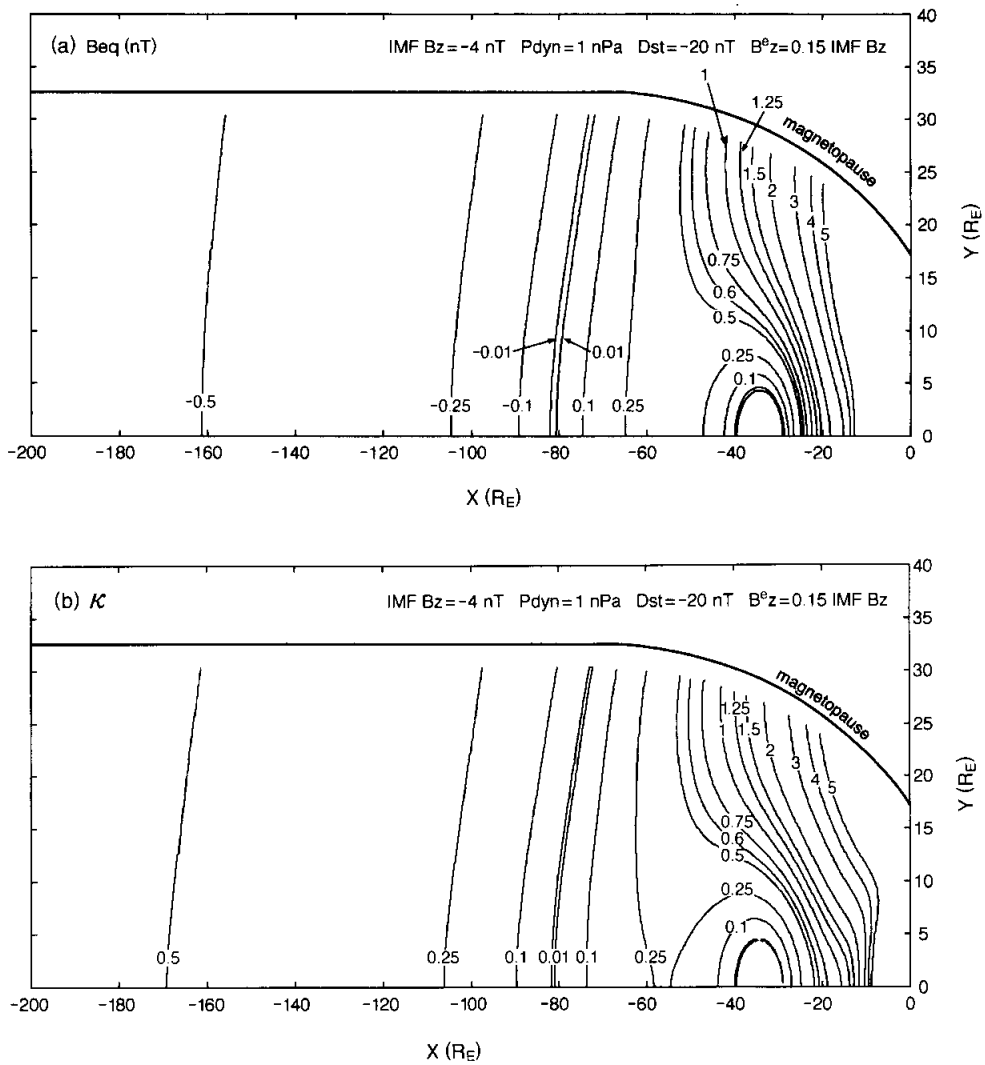

Fig. 3. Equicontours of (a) B_{eq} and (b) κ on the X-Y plane, where IMF $B_Z = -4\,nT$, $P_{dyn} = 1\,nPa$, $D_{ST} = -20\,nT$ and $B_Z^e = 0.15 \times IMF\ B_Z$. (For the definition of κ, see Section 1.) Coordinates X and Y are in units of the Earth radius, R_E.

IMF B_Z is a few nanoteslas; the polar cap is expected to disappear when the B_Z exceeds a certain value between 5 and 9 nT. These facts are also consistent with the aforementioned observation by Makita *et al.* (1988) that the entire polar region is often filled with burst-type soft (< 500 eV) electron precipitation during periods of strongly northward ($B_Z > 5$ nT) IMF; during weakly northward IMF periods, a wide area that does not contain such electron precipitation is present.

In concluding this section, additional comments (a)–(d) are made on the properties of a boundary of the firmly-closed region with regard to particle behavior.

(a) So far, only ion behavior around the nonadiabatic/adiabatic boundary has been

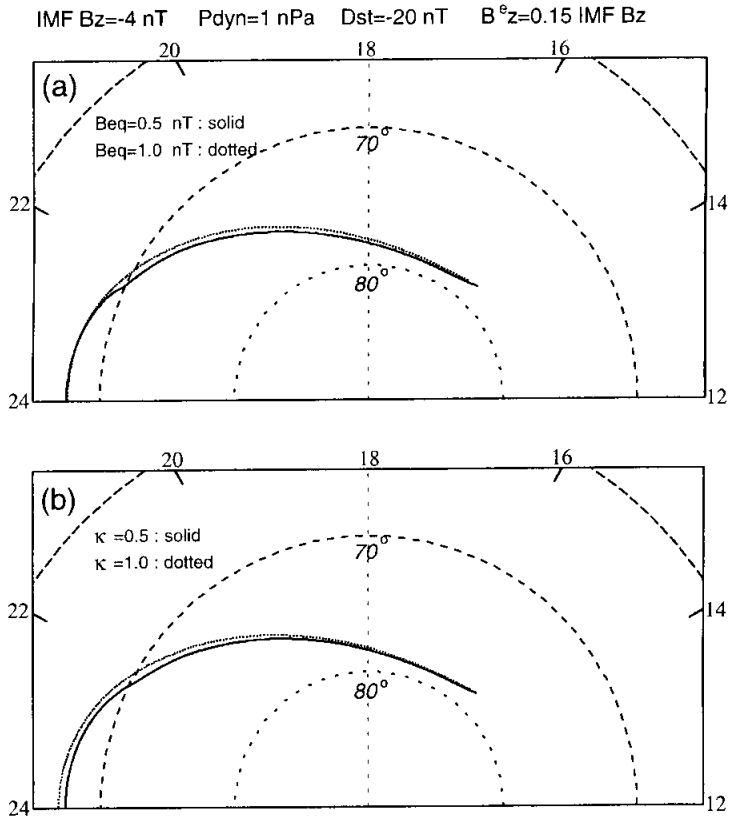

Fig. 4. Ionospheric footprints of (a) $B_{eq}=0.5$ and 1.0 nT lines and (b) $\kappa=0.5$ and 1.0 lines in Fig. 3. The MLT (12 24) dial and the 60°, 70° and 80° magnetic latitude lines are indicated.

considered. Here, possible electron behavior is briefly discussed. As is assumed above, the density of energized ions is higher inside that boundary than outside. In this situation, ions tend to diffuse outwards across the boundary due to anomalous cross-field scattering. The diffusion rate is enhanced by the nonadiabaticity of the ions. For overall charge neutrality, electrons outside the boundary flow along the field lines toward the ionosphere, while the ionospheric electrons just inside the boundary flow away from the ionosphere. Thus, a pair of downward and upward field-aligned currents are generated around the nonadiabatic/adiabatic boundary. As discussed by Yamamoto *et al.* (1997), such field-aligned-currents may lead to an enhancement in auroral luminosity along the poleward edge of the diffuse auroral region, as seen, for example, in the horse-collar aurora (Hones *et al.*, 1989). Another prediction of importance to the present study is that plasma particles, including electrons around that boundary, eventually 'diffuse' toward the outer magnetic shells and tend to escape to interplanetary space, although some of them may be returned by convection.

(b) The parameter of adiabaticity weakly depends on the particle energy; namely, adiabaticity is proportional to $w_{\perp}^{-1/4}$, where $w_{\perp}$ is the ion perpendicular energy. For

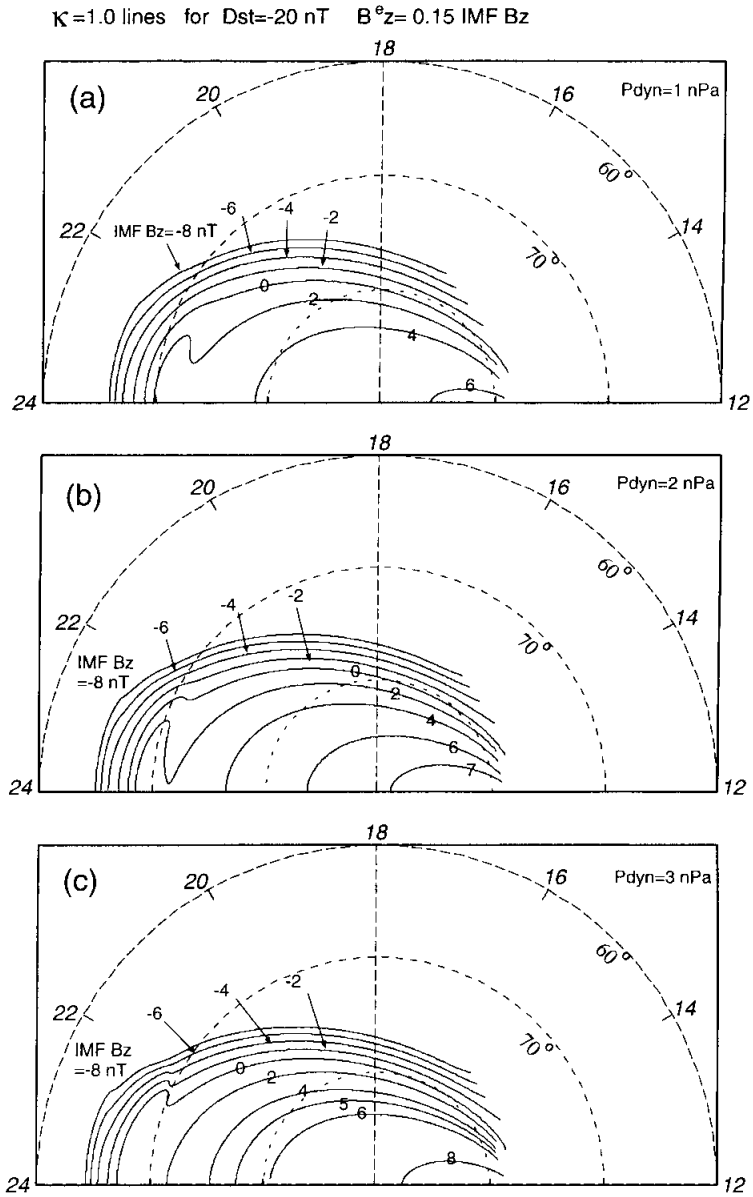

Fig. 5. IMF B_z dependent polar cap: ionospheric footprints of the $\kappa = 1$ lines for various values of IMF B_Z, where (a) $P_{dyn} = 1$ nPa, (b) $P_{dyn} = 2$ nPa and (c) $P_{dyn} = 3$ nPa. In all three cases, $D_{ST} = -20$ nT and $B_z^e = 0.15 \times$ IMF B_Z. (According to satellite observations, the average solar wind dynamic pressure, P_{dyn}, is about 2 nPa (Roelof and Sibeck, 1993). For the statistical distribution of P_{dyn}, see Fig. 4 of their paper.)

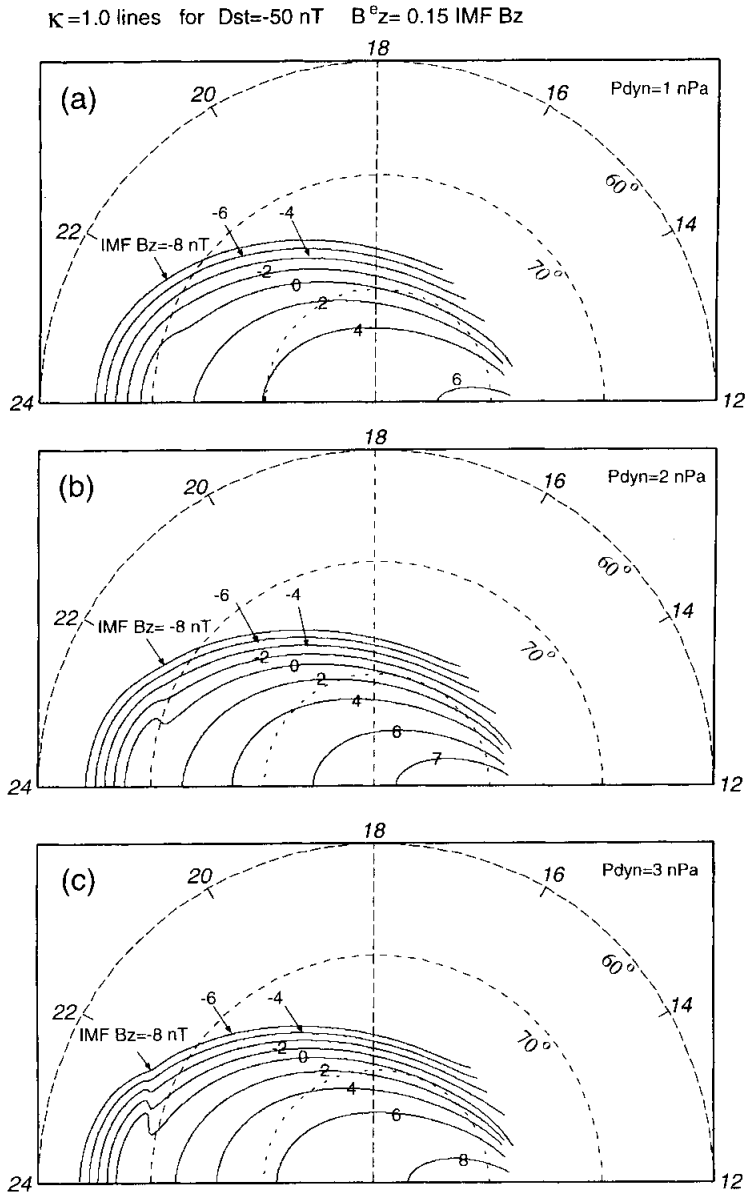

Fig. 6. Same format as Fig. 5, but $D_{ST} = -50$ nT.

example, within a typical energy range of auroral ions ($0.5 < w_{\perp}$ (keV) < 5), the adiabaticity parameter changes only by a factor of 1.8.

(c) The nonadiabatic/adiabatic boundary is not necessarily sharp, even if a single value of particle energy is specified. Boundary sharpness (*i.e.*, the radial or latitudinal scale length) of the 'nonadiabaic to adiabatic' transition is expected to depend on the IMF B_Z under the conditions of steady solar wind and steady magnetosphere. In the case of IMF $B_Z = -4$ nT (see Fig. 4), the $\kappa = 1$ and $\kappa = 0.5$ lines are closely spaced

($<0.5^\circ$ in latitude) on the ionospheric plane, implying a relatively sharp boundary. On the other hand, when IMF $B_Z \gtrsim 0$, the corresponding width is broader because the $\kappa \approx 1$ lines appear at the equator in the distant tail where κ changes slowly with X. For example, in the case of IMF $B_Z = 0$ (the other parameters are the same as in Fig. 4), the spacing of the $\kappa = 1$ and $\kappa = 0.5$ lines is about 3° around midnight, but smaller at other local times.

(d) The $\kappa = 1$ boundary, with κ defined for 1.0 keV ions, is simply a measure of the demarcation between field-line closure and openness as viewed with regard to plasma particles. Despite such simplistic demarcation, the extent of the polar cap presumed from the condition $\kappa = 1$ is consistent with observations, as shown above. The observation of a wide polar cap during weakly northward IMF periods could not be explained using the traditional open/close demarcation based on the neutral line. To develop a more sophisticated model for the open/close demarcation in terms of particle nonadiabaticity will require a numerical simulation for behavior of particles interacting with fluctuating fields in the region of $\kappa \approx 1$. Such theoretical work will be necessary in the future.

4. Magnetic drift velocity on the boundary of firmly-closed region

This section discusses the average magnetic drift velocities of charged particles on the outer boundary of the closed region. The magnetic drift (*i.e.*, gradient B drift plus curvature drift) velocity can be crucial for charge separation near the outer boundary because the energy density of the particles is assumed to change significantly there, during periods of weakly northward to southward IMF. This charge separation is assumed to produce the nightside region 1 field-aligned current (FAC) (see Yamamoto and Inoue (1998)).

Assuming that the plasma pressure, p, is isotropic and uniform along the field lines, the (quasi-steady) FAC density $J_{\parallel i}$ at the ionospheric height is given by the following equation (Yamamoto *et al.*, 1996):

$$J_{\parallel i} = e\bar{v}_{m,i} \cdot \nabla_i \varepsilon, \tag{1}$$

where e (>0) is the electronic charge, ∇_i denotes the gradient on the ionospheric plane, and the positive value of $J_{\parallel i}$ is for the FAC flowing away from the ionosphere, *i.e.*, the upward FAC. Here, ε is the flux tube energy content, which is defined as the total kinetic energy of plasma particles contained in a flux tube with unit cross-sectional area at the ionospheric height:

$$\varepsilon = \int_{s_i}^{s_e} \frac{3p}{2} \frac{B_i}{B(s)} ds.$$

The average value of the ionospheric projection of the magnetic drift velocity per unit energy, which is defined as follows:

$$\bar{v}_{m,i} = \frac{1}{R_b} \int_{s_i}^{s_e} \frac{V_{m,i}(s)}{W} \frac{B_i}{B(s)} ds \quad \text{and} \quad R_b = \int_{s_i}^{s_e} \frac{B_i}{B(s)} ds, \tag{2}$$

where $V_{m,i}(s)$ is the ionospheric projection of the magnetic drift velocity of the proton

fluid with average energy W; s is the field-aligned distance, and s_e and s_i are the field-aligned distances at the equator and the ionospheric height, respectively; $B(s)$ and B_i are the magnetic field strengths at the distances s and s_i, respectively. The quantity R_b represents the volume of a flux tube with unit cross-sectional area at the ionospheric height. The velocity $\bar{v}_{m,i}$ is derived from the gradient of R_b (Vasyliunas, 1970; Yamamoto *et al.*, 1996):

$$\bar{v}_{m,i} = -\frac{2}{3e}\frac{1}{R_b B_i}\boldsymbol{b}_i \times \nabla_i R_b, \tag{3}$$

where $\boldsymbol{b}_i$ is the unit vector parallel to the ionospheric magnetic field $\boldsymbol{B}_i$. Neglecting the local time dependence of the flux tube energy content ε along the outer boundary of the closed region (see Section 3 of Y99), the current density $J_{\perp i}$ on the boundary is determined by the component of $\bar{v}_{m,i}$ perpendicular to it as well as the perpendicular gradient of ε (see eq. (1)). Integrating $J_{\perp i}$ across the boundary (in the perpendicular direction), the FAC intensity, I, is approximately given by the following equation:

$$I \sim e(\bar{v}_{m,i})_{\perp}[\varepsilon], \tag{4}$$

where $(\bar{v}_{m,i})_{\perp}$ is the equatorward component (perpendicular to the boundary) of $\bar{v}_{m,i}$, and $[\varepsilon]$ is the net change (>0) of ε across the boundary. From eqs. (3) and (4), the intensity I is found to be proportional to the gradient R_b along the boundary:

$$I \propto [\varepsilon]\frac{\partial}{\partial l}\ln R_b, \tag{5}$$

where l is the boundary-aligned distance on the ionospheric plane. By using the term "distortion" to refer to $\partial R_b/\partial l \neq 0$ (Yamamoto and Inoue, 1998), the production of the region 1 FAC can be said to depend on the distortion of the outer boundary of the closed region.

In Fig. 7, the equicontours of R_b are plotted on the equatorial plane for the case of IMF $B_Z=0$, $P_{\mathrm{dyn}}=1$ nPa and $D_{\mathrm{ST}}=-20$ nT. Here, R_b is normalized by the value of R_b, R_{b0}, for the dipole field line with an equatorial distance of 7 Earth radii: $R_{b0}=1.32\times10^{10}$ m. The contour of $\kappa=1$ is superposed on the figure. From this figure, R_b is found to change greatly along the $\kappa=1$ line, *i.e.*, the outer boundary of the closed region. Figure 8 shows more explicitly how the flux tube volume R_b on the $\kappa=1$ line varies with MLT (magnetic local time) for various IMF B_Z in the case of $P_{\mathrm{dyn}}=1$ nPa and $D_{\mathrm{ST}}=-20$ nT. For all the cases shown in Fig. 8, R_b on the $\kappa=1$ line is minimized around midnight and increases toward dusk or dawn. For IMF $B_Z\leq2$, the total increase of R_b in the interval between 24 and 18 MLT is greater than a factor of 7. As was discussed in the appendix of Y99, this increase in R_b can essentially be attributed to the increase in the field-line length.

In Fig. 9, the perpendicular components of $\bar{v}_{m,i}\times(1\,\mathrm{keV})$ on the $\kappa=1$ line are plotted for IMF $B_Z=-4$ nT (Fig. 9a), IMF $B_Z=0$ (Fig. 9b), and IMF $B_Z=4$ nT (Fig. 9c) in the case of $P_{\mathrm{dyn}}=1$ nPa and $D_{\mathrm{ST}}=-20$ nT. As is expected from the gradients of R_b in Fig. 8 (see also eq. (3)), $(\bar{v}_{m,i})_{\perp}$ is directed equatorward on the duskside and poleward on the dawnside. Consequently, FACs in region 1 sense can be generated around the outer boundary of the closed region when the flux tube energy content ε has

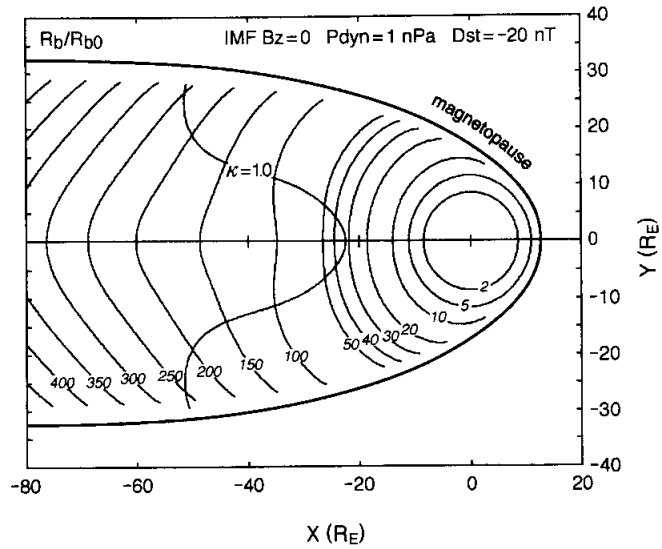

Fig. 7. Equicontours of the flux tube volume R_b normalized by R_{b0} (for definitions, see text) on the equatorial plane, where IMF $B_Z=0$, $P_{dyn}=1$ nPa and $D_{ST}=-20$ nT. The $\kappa=1$ line is superposed on the figure.

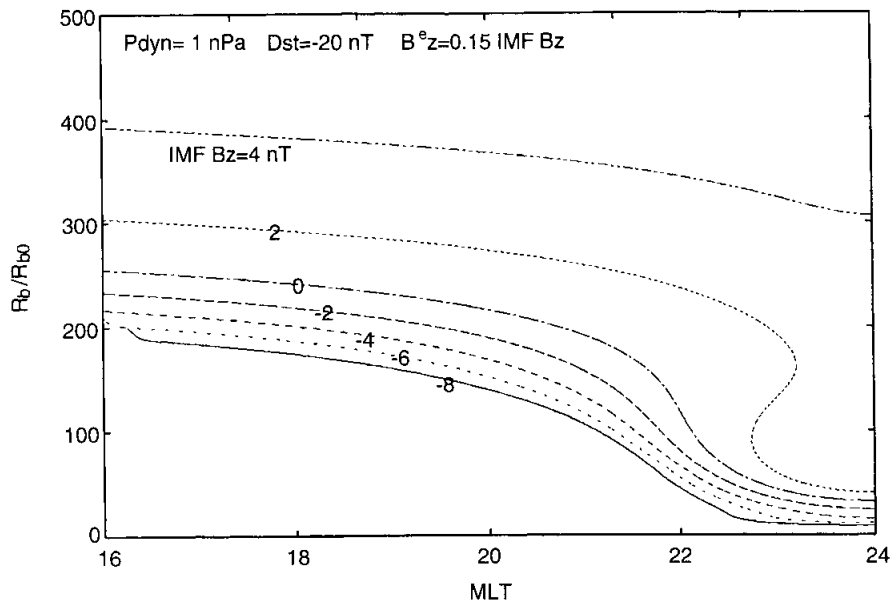

Fig. 8. Variations of the flux tube volume $R_b=R_{b0}$ along the $\kappa=1$ line (in Fig. 5a), for various values of IMF B_Z, where $P_{dyn}=1$ nPa, $D_{ST}=-20$ nT and $B'_Z=0.15\times$IMF B_Z.

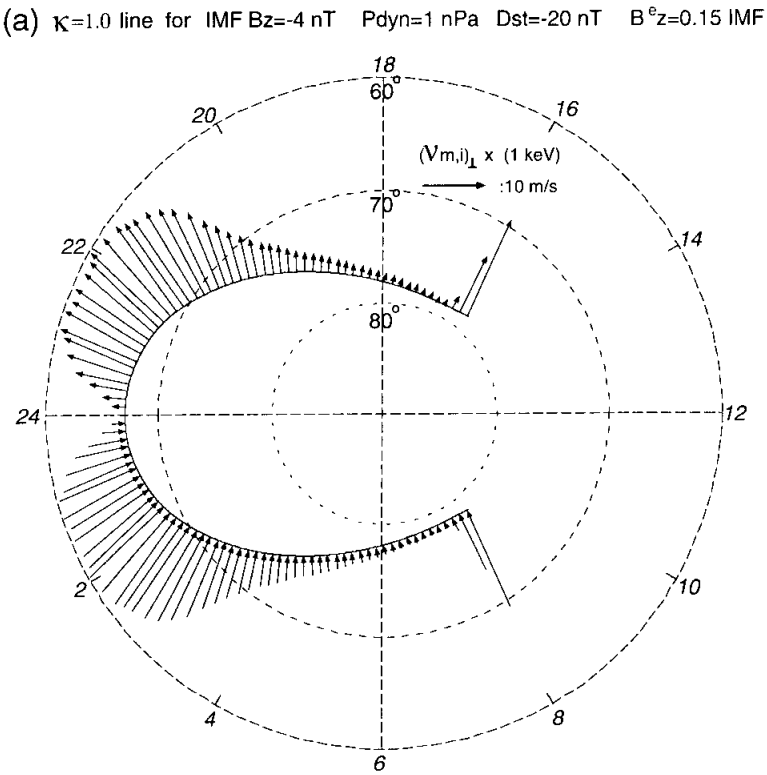

Fig. 9. Perpendicular (to the $\kappa=1$ line) component of the average magnetic drift velocity, $(\bar{v}_{m,i})_\perp \times (1\,keV)$, projected to the ionosphere, for an ion fluid with an isotropic pressure and average energy of 1 keV is plotted along the $\kappa=1$ line (in Fig. 5a). (a) IMF $B_Z=-4\,nT$, (b) IMF $B_Z=0$ and (c) IMF $B_Z=4\,nT$. For all cases, $P_{dyn}=1\,nPa$, $D_{ST}=-20\,nT$ and $B^e_Z=0.15\times IMF\ B_Z$.

an equatorward gradient at that location. As a numerical example, suppose that $R_b/R_{b0}\sim 100$ and $|(\bar{v}_{m,i})_\perp|\sim 15\,m/s/keV$, and that the number density and the average energy of the plasma particles just inside the boundary are $0.04\,cm^{-3}$ and 3 keV, respectively. Then $[\varepsilon]\sim 0.12\ (keVcm^{-3})\times 100R_{b0}$, and finally the FAC intensity in eq. (4) is estimated as $I\sim 0.4\,A/m$. This value is comparable to a typical intensity ($\gtrsim 0.1$ A/m) of the region 1 FACs observed near the poleward edge of the region of auroral particle precipitation (*e.g.*, Fukunishi *et al.*, 1993). Notably, the recent analysis of magnetic field perturbation measured from the EXOS-D satellite (Yamamoto *et al.*, 1999b) has revealed that the region 1 FAC is often concentrated into a narrow ($\sim 0.5^\circ$ in latitude) zone near the poleward edge of the auroral oval.

Finally, Fig. 10 shows how widely (in the parameter range) the boundary distortion occurs: the ratio between the two values of R_b at MLT = 18 and 24 hours on the same $\kappa=1$ line is plotted against IMF B_Z for $P_{dyn}=1$, 2 and 3 nPa in the cases of (a) $D_{ST}=-20\,nT$ and (b) $D_{ST}=-50\,nT$. In case (b), the degree of distortion, *i.e.*, R_b (MLT = 18)/R_b (24) is less than in case (a) under the same IMF (and P_{dyn}) conditions. This may be understood from the following fact: the more developed ring current in the

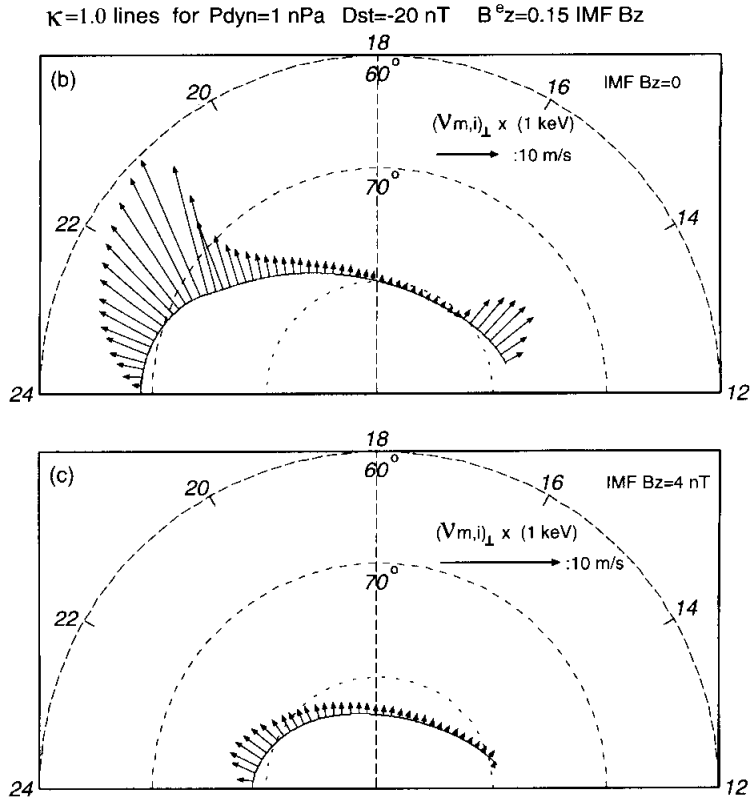

Fig. 9. Continued.

case with the lower D_{ST} increases the equatorial magnetic field outside of the ring current zone. The parameter κ is then increased in the outer magnetic shells, but this increment is smaller in the more distant regions. Therefore, in the midnight sector, the $\kappa = 1$ line for the lower D_{ST} is located farther from the Earth than that for the higher D_{ST}, meaning a higher value of R_b (MLT = 24) on the $\kappa = 1$ line for the lower D_{ST}. Since R_b (18) is insensitive to the D_{ST} value, a smaller ratio of R_b (MLT = 18)/R_b (24) is obtained for the lower D_{ST}. In passing, note that the smaller degree of distortion in the case with the lower D_{ST} does not necessarily mean the generation of weaker region 1 currents because a higher level of flux tube energy content, ε, would generally be expected in such a case.

From Fig. 10 it is found that the distortion is a general property of the outer boundary of the closed region, and that when the IMF B_Z is comparable to or less than 1 nT, the boundary distortion is significant enough to generate region 1 field-aligned currents with observable intensities via a pressure gradient mechanism.

5. Conclusions

This paper proposes that the outer boundary of the firmly-closed region should be represented by field lines with the parameter of adiabaticity, κ, equal to unity at the

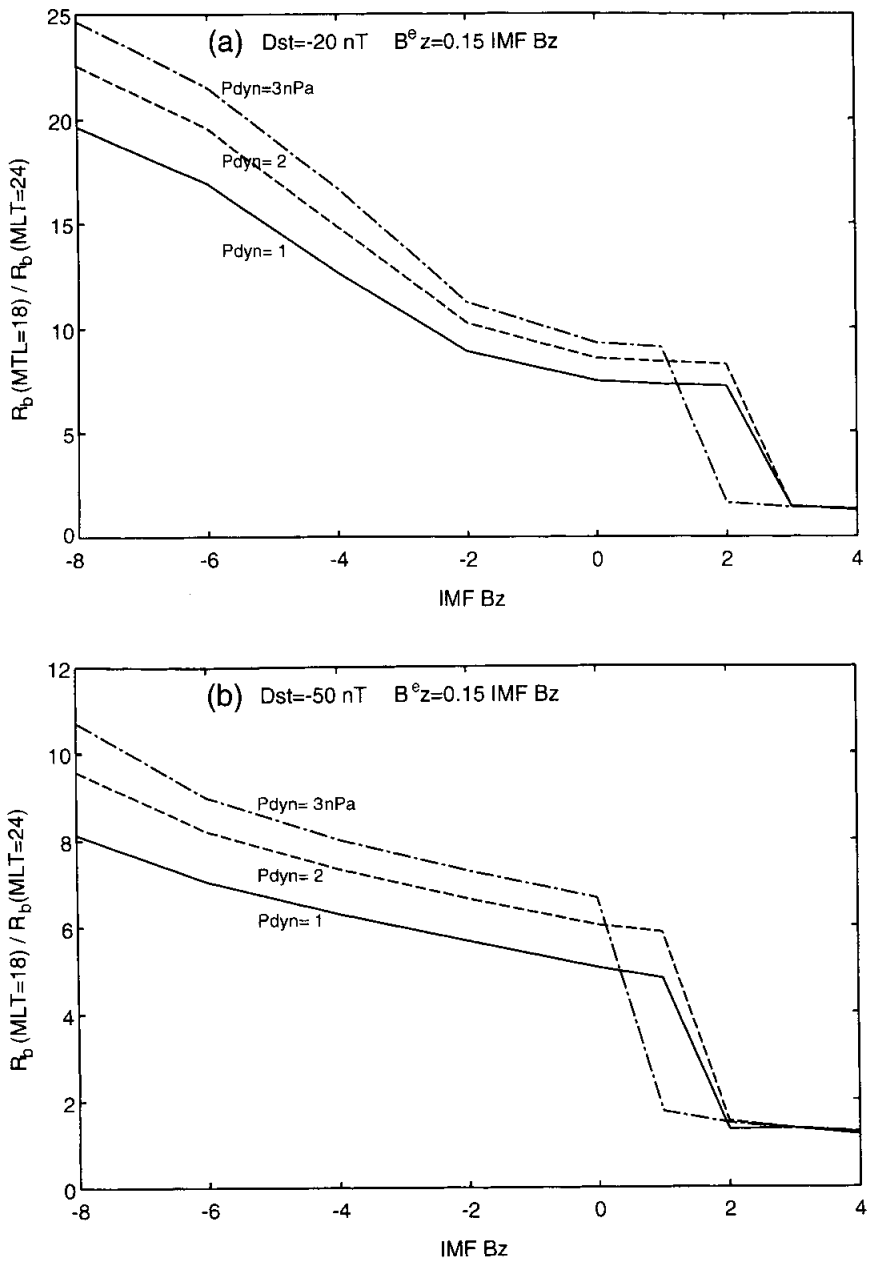

Fig. 10. Ratio between the two values of R_b at MLT=18 and 24 hours, on the same $\kappa=1$ line, plotted against IMF B_Z for $P_{dyn}=1$, 2 and 3 nPa in the cases of (a) $D_{ST}=-20$ nT and (b) $D_{ST}=-50$ nT; $B_Z^e=0.15\times$IMF B_Z.

equator. The outer boundary can be numerically determined using the Tsyganenko magnetic field model (1996). To include the penetration effect of IMF B_Z, 15 % of the IMF B_Z (a parameter in the original T96 model) is uniformly added to the original field. The outer boundary of the firmly-closed region in this modified model has the following characteristics: (1) the size of the polar cap (defined to be encircled by the $\kappa=1$ boundary) on the ionosphere expands with decreasing IMF B_Z, (2) a wide polar cap exists when IMF $B_Z \simeq 1$ nT, and the polar cap disappears as B_Z exceeds a certain level between 5 and 9 nT, and (3) the outer boundary of the closed region is significantly distorted when IMF B_Z is comparable to or less than 1 nT, enabling region 1 field-aligned currents with observable intensities to be generated by a pressure gradient mechanism. These characteristics are all consistent with actual observations. Finally, it should be emphasized that fact (2) cannot be explained using the traditional open/close demarcation based on the neutral line.

Acknowledgments

The work of T. Yamamoto was supported in part by the joint research programs at Radio Atmospheric Science Center, Kyoto University, Uji, Kyoto, the Institute of Space and Astronautical Science, Sagamihara, Kanagawa, and the National Institute of Polar Research, Itabashi, Tokyo.

The editor thanks Dr. T. Pulkkinen and another referee for their help in evaluating this paper.

References

Akasofu, S.-I., Meng, C.-I. and Makita, K. (1992): Changes of the size of the open field line region during substorms. Planet. Space Sci., **40**, 1513–1524.

Ashour-Abdalla, M., Zelenyi, L.M., Peroomian, V., Richard, R.L. and Bosqued, J.M. (1995): The mosaic structure of plasma bulk flows in the Earth's magnetotail. J. Geophys. Res., **100**, 19191–19209.

Birn, J., Hones, E.W., Jr., Craven, J.D., Frank, L.A., Elphinstone, R.D. and Stern, D.P. (1991): On open and closed field line regions in Tsyganenko's field model and their possible associations with horse collar auroras. J. Geophys. Res., **96**, 3811–3817.

Bühner, J. and Zelenyi, L.M. (1989): Regular and chaotic charged particle motion in magnetotaillike field reversals 1. Basic theory of trapped motion. J. Geophys. Res., **94**, 11821–11842.

Cowley, S.W.H. and Hughes, W.J. (1983): Observation of an IMF sector effect in the Y magnetic field component at geostationary orbit. Planet. Space Sci., **31**, 73–90.

Elphinstone, R.D., Hearn, D., Murphree, J.S. and Cogger, L.L. (1991): Mapping using the Tsyganenko magnetic field model and its relationship to Viking auroral images. J. Geophys. Res., **96**, 1467–1480.

Fairfield, D.H. (1979): On the average configuration of the geomagnetic tail. J. Geophys. Res., **84**, 1950–1958.

Fukunishi, H., Takahashi, Y., Nagatsuma, T., Mukai, T. and Machida, S. (1993): Latitudinal structures of nightside field-aligned currents in their relationships to the plasma sheet regions. J. Geophys. Res., **98**, 11235–11255.

Hones, E.W., Jr., Craven, J.D., Frank, L.A., Evans, D.S. and Newell, P.T. (1989): The horse-collar aurora: a frequent pattern of the aurora in quiet times. Geophys. Res. Lett., **16**, 37–40.

Lin, N., McPherron, R.L., Kivelson, M.G. and Walker, R.J. (1991): Multipoint reconnection in the near-Earth magnetotail: CDAW 6 observations of energetic particles and magnetic field. J. Geophys. Res., **96**, 19427–19439.

Makita, K., Meng, C.-I. and Akasofu, S.-I. (1988): Latitudinal electron precipitation patterns during large and small IMF magnitudes for northward IMF conditions. J. Geophys. Res., **93**, 97–104.

Nishitani, N. (1992): Magnetic field line connection between the ionosphere and the magnetosphere-auroral activity and relevant magnetic field variation at geosynchronous orbit. Ph. D Thesis for Nagoya Univ.

Roelof, E.C. and Sibeck, D.G. (1993): Magnetopause shape as a bivariate function of interplanetary magnetic field B_Z and solar wind dynamic pressure. J. Geophys. Res., **98**, 21421–21450.

Tsyganenko, N.A. (1987): Global quantitative models of the geomagnetic field in the cislunar magnetosphere for different disturbance levels. Planet. Space Sci., **35**, 1347–1358.

Tsyganenko, N.A. (1989): A magnetospheric magnetic field model with a warped tail current sheet. Planet. Space Sci., **37**, 5–20.

Tsyganenko, N.A. (1995): Modeling the Earth's magnetospheric magnetic field confined within a realistic magnetopause. J. Geophys. Res., **100**, 5599–5612.

Tsyganenko, N.A. and Stern, D.P. (1996): Modeling the global magnetic field of the large-scale Birkeland current systems. J. Geophys. Res., **101**, 27187–27198.

Usadi, A., Kageyama, A., Watanabe, K. and Sato, T (1993): A global simulation of the magnetosphere with a long tail: southward and northward interplanetary magnetic field. J. Geophys. Res., **98**, 7503–7517.

Vasyliunas, V.M. (1970): Mathematical models of magnetospheric convection and its coupling to the ionosphere. Particles and Fields in the Magnetosphere, ed. by B.M. McCormac. Norwell, D. Reidel, 60–71.

Yamamoto, T. and Inoue, S. (1998): Quasi-steady production of region 1 and region 2 field-aligned currents. Proc. NIPR Symp. Upper Atmos. Phys., **11**, 106–120.

Yamamoto, T., Inoue, S., Nishitani, N., Ozaki, M. and Meng, C.-I. (1996): A theory for generation of the paired region 1 and region 2 field-aligned currents. J. Geophys. Res., **101**, 27199–27222.

Yamamoto, T., Inoue, S. and Meng, C.-I. (1997): Effect of anomalous cross-field diffusion on the field-aligned current generation. J. Geomagn. Geoelectr., **49**, 923–945.

Yamamoto, T., Inoue, S., Ozaki, M. and Nishitani, N. (1999a): Distortion of the outer boundary of the closed region in the Tsyganenko magnetic field model. Adv. Polar Upper Atmos. Res., **13**, 89–104.

Yamamoto, T., Inoue, S. and Ozaki, M. (1999b): Latitudinal structure of the nightside region 1 field-aligned current observed from the EXOS-D satellite. Adv. Polar Upper Atmos. Res., **13**, 105–118.

(Received September 26, 2000; Revised manuscript accepted March 16, 2001)